Article:
Hua, H., Zhu, Z.Q. orcid.org/0000-0001-7175-3307, Pride, A. et al. (2 more authors) (2017) A Novel Variable Flux Memory Machine With Series Hybrid Magnets. IEEE Transactions on Industry Applications, 53 (5). pp. 4396-4405. ISSN 0093-9994

https://doi.org/10.1109/TIA.2017.2709261

A Novel Variable Flux Memory Machine with Series Hybrid Magnets

Hao Hua, Z.Q. Zhu
Department of Electronics and Electrical Engineering
University of Sheffield, Sheffield, S1 3JD, U.K.

Adam Pride, Rajesh Deodhar, Toshinori Sasaki
IMRA Europe S.A.S. U.K. Research Center
Brighton, BN1 9RS, U.K.

***Abstract*—This paper proposes a novel variable flux memory (VFM) machine, in which the "constant" permanent magnet (PM) (CPM) with high coercive force and the "variable" PM (VPM) with low coercive force are alternatively located in the interior-PM (IPM) rotor. Thus, the VPMs and CPMs are magnetically connected in series, with which the CPMs can assist the VPMs to withstand the unintentional demagnetization caused by armature reaction. Therefore, a high armature current can be applied to the machine. Meanwhile, the reluctance torque is retrieved. Thus, a high torque density can be obtained. Based on two-dimensional (2-D) finite element (FE) analysis, the electromagnetic performance of the proposed VFM machine in two extreme magnetization states is firstly evaluated in detail. Then, the demagnetization and re-magnetization characteristics are investigated, in which the working points of VPMs are illustrated. Furthermore, the advantages of improved efficiency of the proposed VFM machine are demonstrated. A prototype machine is manufactured and tested to validate the predictions.**

Keywords—effciency; memory machine; permanent magnet; series connection; torque; variable flux

I. INTRODUCTION

Permanent magnet (PM) machines benefit from high torque density and high efficiency, which have been extensively investigated and employed [1], [2]. Nevertheless, their relatively constant air-gap flux makes the effective flux-weakening operation become a challenge, which has restricted their applications in variable-speed systems. Many investigations have been carried out to enhance the flux-weakening capability of PM machines. The vector control principle has been successfully applied, and a negative *d*-axis armature current ($-i_d$) is injected to counter the PM flux and thus effectively reduce the induced voltage [3], [4]. However, $-i_d$ is continuously required to conduct the flux-weakening control, which expends armature current capacity and produces extra copper loss. Besides, the dual-part rotor technique has been presented [5], [6], in which a reluctance rotor and a surface-mounted PM rotor are axially combined, together with one common stator. As a consequence, the machine saliency ratio is increased and the flux-weakening capability is improved. Nevertheless, the machine robustness and torque density are sacrificed.

Therefore, variable flux memory (VFM) machines have been proposed to offer an alternative solution [7], in which the low coercive force PM, i.e. variable PM (VPM), is employed. In [7], [8], the tangentially magnetized VPMs are inserted in the rotor, and their magnetization state can be varied by a current pulse, while dissipating negligible copper loss. As a result, the PMs are flexibly controlled to obtain the most appropriate state for each operation point, and hence the flux-weakening can be easily achieved. In VFM machines, i_d is employed to vary the magnetization state of VPMs while *q*-axis current (i_q) is simultaneously used for torque generation.

In [9], [10], based on the flux-intensifying interior-PM (IPM) machines which are characterized with a saliency ratio greater than one, i.e. *d*-axis inductance (L_d) is higher than *q*-axis inductance (L_q) due to *q*-axis flux barriers in the rotor, the corresponding VFM machines are presented. Consequently, the positive reluctance torque is obtained with $+i_d$ while the magnetization state of VPM can be stabilized simultaneously, avoiding unintentional demagnetization. The benefits of these VFM machines in improving efficiency are evaluated in [11]. Moreover, the spoke-type IPM rotor has been employed to boost the PM usage volume and hence the torque output [12], [13]. However, these VFM machines still suffer sacrificed torque densities due to the employment of weak VPMs and complicated flux barriers. Alternatively, stator-PM machines incorporated with the VFM concept have been presented [14]-[17], in which an additional field winding on the stator is required to control the DC current for magnetization and demagnetization. Thus, the torque density is further sacrificed due to space conflict in the stator.

To improve the torque density of VFM machines, the hybrid PM topologies in which both VPM and constant PM (CPM) with high coercive force, e.g. NdFeB, are employed, have been developed [18]. The CPMs provide a constant field whilst the VPMs offer an additional variable component. The variation of PM flux is still achievable, and meanwhile, the torque density is boosted thanks to the employment of CPMs. In [18]-[20], the VPMs and CPMs are located on the same rotor pole with parallel magnetic circuits. However, the cross-coupling between two types of PMs is severe in these parallel hybrid PM VFM machines, in which the CPMs tend to automatically demagnetize the VPMs and thus the working point of VPMs is very difficult to hold [21]. In addition, in order to avoid the unintentional demagnetization, i_d is seldom used during torque generation and thus the reluctance torque is absent. A fractional-slot VFM machine with VPMs and CPMs alternatively surface-mounted on the rotor, is

investigated, in which all VPMs are magnetized with the identical polarity while all CPMs have the other identical polarity [22], [23]. Therefore, two types of PMs are magnetically connected in series. The CPM flux can assist the VPM to withstand the unintentional demagnetization, and the harmful cross-coupling is greatly alleviated. Nevertheless, due to the surface-mounted PMs and the fractional-slot stator structure, the reluctance torque is still absent and the torque capability is limited in this machine.

To the best of authors' knowledge, up to date, the torque densities of the existing VFM machine topologies are always sacrificed, which are normally lower than 20kNm/m^3. To boost the torque density of VFM machines, a novel series hybrid PM VFM machine, which employs full-pitched windings and a V-shaped IPM rotor with alternatively placed VPMs and CPMs, is proposed and investigated in this paper. The novel machine inherits the feature of variable flux and benefits from the improved torque density [24].

The paper is organized as follows. In section II, the topology and operating principle of the proposed VFM machine are described, with particular attention to the advantages of series hybrid PM structures. Then, in section III, the electromagnetic performance of the novel VFM machine is comprehensively evaluated based on two-dimensional (2-D) finite element (FE) analysis. The characteristics of demagnetization and re-magnetization are illustrated in section IV, followed by the analysis of efficiency improvement in section V. Finally, a prototype machine is manufactured and the experimental validation is carried out in section VI.

II. Machine Topology and Operating Principle

The proposed series hybrid PM VFM machine is illustrated in Fig. 1, in which the three-phase 48-stator-slot/8-rotor-pole structure that is similar to the commercial Toyota Prius2010 IPM machine is employed. The full-pitched armature winding and IPM rotor are employed to obtain the reluctance torque, and the V-shaped PMs are employed to improve the available PM flux. Moreover, the CPMs and VPMs are alternatively located on different rotor poles, i.e. one rotor pole is composed of CPMs while the adjacent pole consists of VPMs. All CPMs are magnetized with the identical polarity while all VPMs have the other polarity. As a result, the CPMs and VPMs are magnetically connected in series.

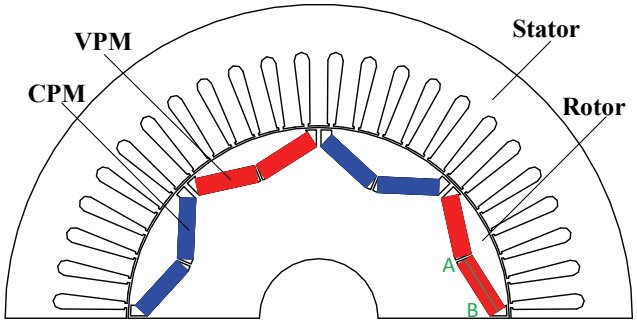

Fig. 1 Cross section of the proposed series hybrid PM VFM machine.

A. Operation of VPM

The feature of variable magnetization in VFM machines depends on the characteristics of VPMs. Fig. 2 shows the operation of the VPM under open-circuit conditions. Due to the non-linear B-H curve in Quadrant II, the magnetization state of the VPM is easy to vary by an external field. For instance, based on the initial working point A, it will shift to point B that is lower than the knee point if a large demagnetization magnetomotive force (MMF) is applied. Then, the working point will move along the recoil line BD and terminate at point C when the negative MMF is released. Afterwards, if a magnetization MMF pulse is applied, the working point can shift to point F along the curve CDEF, which indicates the re-magnetization has been conducted. Consequently, it can be found that the working point of the VPM can be flexibly varied by applying different MMF pulses.

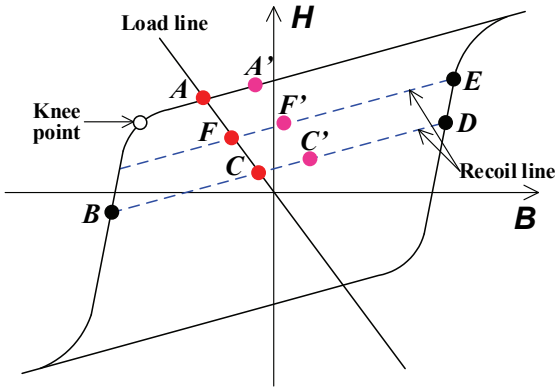

Fig. 2 Illustration of the operation of VPM (B: flux density, H: magnetic field strength).

B. Series connection

The proposed VFM machine features with a series magnetic connection between VPMs and CPMs. The magnetic circuit of series connection can be simplified in Fig. 3(a), where F_{CPM}, F_{VPM}, R_{m_CPM}, and R_{m_VPM} represent the equivalent MMFs and intrinsic reluctance of CPM and VPM respectively, whilst R_{m_d} is the equivalent external d-axis reluctance. It can be seen that the CPM flux has to go through the VPM, and hence it naturally assists the VPM to withstand the unintentional demagnetization caused by armature reaction. In fact, the VPM working points as shown in Fig. 2 would actually shift from points A, C, F to points A', C', F' respectively, when the CPMs are present in a series hybrid PM connection. Therefore, the flux density in the VPM is enhanced by the CPM, and it becomes more stable. In contrast, as the conventional parallel connection shown in Fig. 3(b) [15]-[17], the CPM flux potentially short-circuits via VPM branch, and it cannot help VPM to withstand the unintentional demagnetization. The CPM even demagnetizes the VPM if two branches are not balanced. Consequently, the working point of the VPM with parallel hybrid PM connection would be lower than that without CPM, indicating that the VPM may be very easily demagnetized in parallel hybrid PM VFM machines.

As the series hybrid PM VFM machines inherently benefit from an improved capability of resisting unintentional demagnetization, the complicated flux barriers employed to alleviate cross-coupling and prevent demagnetization in the conventional VFM machines [6]-[9], [16], can be avoided. This greatly eases the machine design and improves the mechanical strength. More importantly, $-i_d$ turns to be acceptable during torque generation, with which the reluctance torque can be obtained.

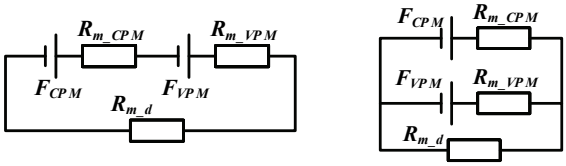

(a) Series (b) Parallel

Fig. 3 Illustration of connection types between VPM and CPM.

III. Electromagnetic Performance in Two Typical Magnetization States

Based on 2-D FE analysis, the electromagnetic performance of the proposed VFM machine is comprehensively evaluated, in which two typical states, i.e. VPM fully forward or fully reverse magnetized, are illustrated. The key design parameters of the machine are listed in Table I, in which the stator and armature windings are the same as the Prius2010 IPM machine. The SmCo and NdFeB PM materials are used as VPM and CPM respectively.

Table I.
Key design parameters of proposed VFM machine.

Parameter	Value
Phase number	3
Slot number	48
Pole number	8
Axial length	50.8 mm
Stator outer diameter	264 mm
Stator inner diameter	161.9 mm
Rotor outer diameter	160.44 mm
Rotor inner diameter	68 mm
Air-gap length	0.73 mm
Steel grade	35H270
Number of turns per coil	11
Number of coils per phase	8
CPM B_r	1.2 T
CPM H_c	915 kA/m
CPM thickness	6.5 mm
VPM B_r	1.14 T
VPM H_c	335 kA/m
VPM thickness	7 mm
Rated current density	26.8 A/mm^2

The open-circuit field distributions in the two magnetization states are presented in Fig. 4. The VPMs are outward magnetized and CPMs are inward magnetized in the fully forward magnetization state, while all PMs are inward magnetized in the fully reverse state. Obviously, the flux is easy to pass through the VPMs and higher flux densities can be observed in the forward magnetization state, as shown in Figs. 4(a) and (c). In contrast, in the fully reverse magnetization state, although the CPMs are strong enough to counter the VPMs and make the flux flow outward in the VPMs, the resultant flux densities are significantly lower than the first state. Meanwhile, the flux lines prefer to bypass the VPMs and thus the magnetic saturation is severe in the rotor iron bridges.

Furthermore, the open-circuit radial flux densities on air-gap are compared in Fig. 5, in which the waveforms in the fully forward state is entirely higher than the fully reverse state, and a much higher fundamental value can be found. The significant difference in amplitudes between the air-gap flux densities in the two states implies the capability of a wide range of flux variation. Meanwhile, since flux density periods are kept the same in the two states, the rotor pole-pair number is unchanged even the VPMs are reversely magnetized.

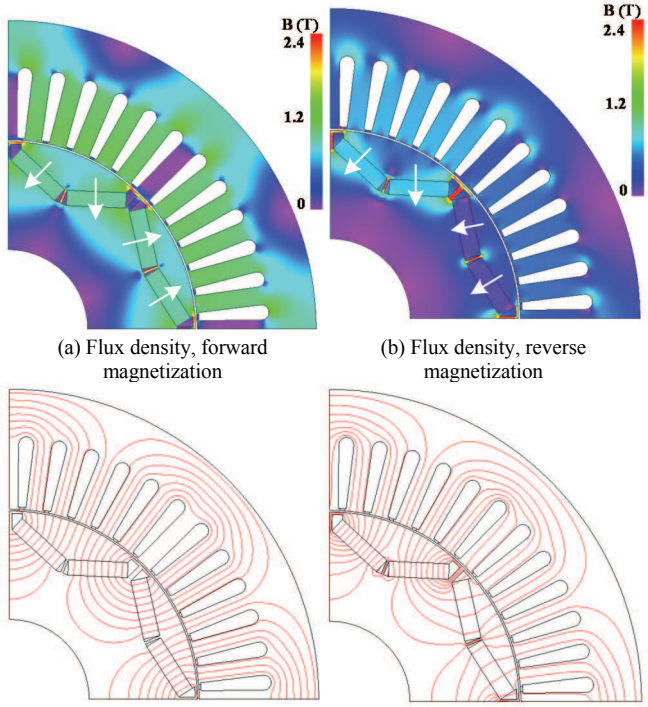

(a) Flux density, forward magnetization (b) Flux density, reverse magnetization

(c) Flux line, forward magnetization (d) Flux line, reverse magnetization

Fig. 4 Open-circuit field distributions in fully forward and reverse magnetization states.

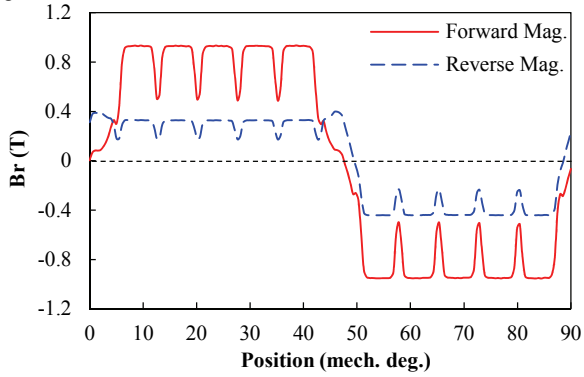

(a) Waveforms

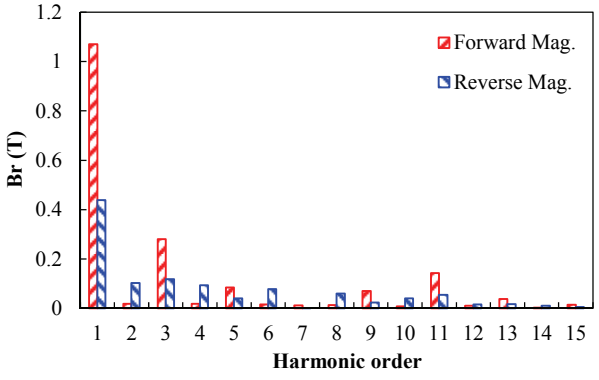

(b) Spectra

Fig. 5 Open-circuit air-gap radial flux densities in fully forward and reverse magnetization states.

The phase back electromotive-forces (back-EMFs) at 1500 r/min in the two states are shown in Fig. 6. The corresponding fundamental amplitudes are 117V and 48V in the forward and reverse states respectively, revealing that a maximum available flux variation range between 41% and 100% can be achieved.

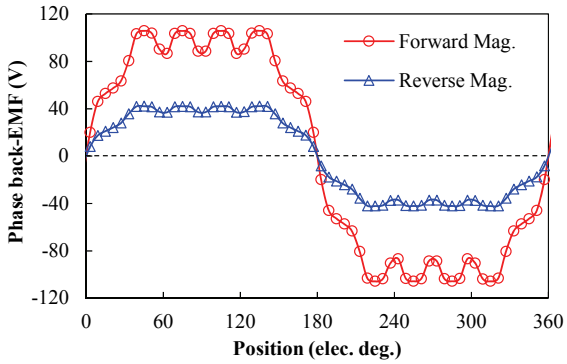

(a) Waveforms

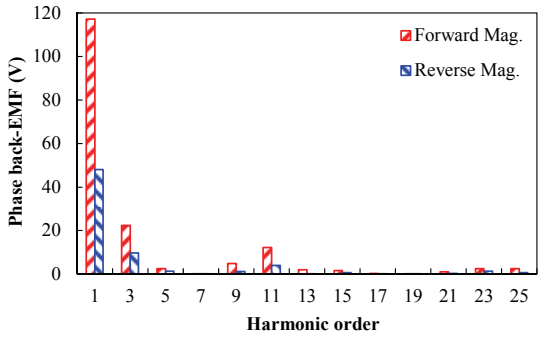

(b) Spectra

Fig. 6 Open-circuit phase back-EMFs at 1500 r/min in fully forward and reverse magnetization states.

The cogging torques in the fully forward and reverse magnetization states are shown in Fig. 7. As the rotor pole-pair number is constant in different states, the cycle numbers of cogging torque are identical. However, the amplitude of cogging torque in the forward state is remarkably higher due to the stronger magnetic field.

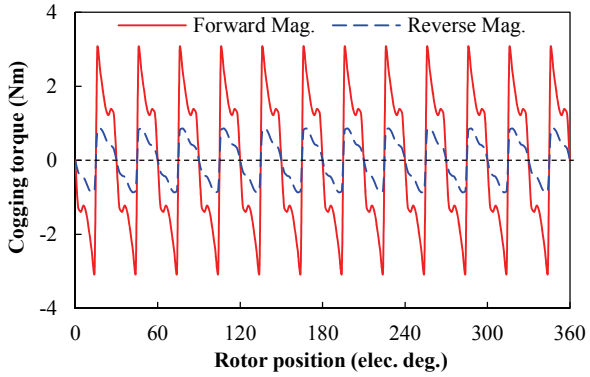

Fig. 7 Cogging torques in fully forward and reverse magnetization states.

Compared to the conventional VFM machines, the high torque density is a major advantage of the proposed VFM machine, which will be analyzed in detail. Fig. 8 illustrates the average torque versus current angle (the phase angle between phase current and open-circuit back-EMF), with the rated current amplitudes of 236A. It can be observed that the peak torque approximately occurs at 40° in the forward magnetization state, and a significant reluctance torque (around 25% compared with the total torque output) is obtained. Thanks to the series magnetic connection of CPMs and VPMs, the capability of resisting unintentional demagnetization is greatly improved. It is safe to apply $-i_d$ and thus the reluctance torque is retrieved. Consequently, a feature of IPM machines, viz. existence of reluctance torque, is inherited in the proposed VFM machine, which benefits the overall torque density. The torque output is significantly lower in the reverse magnetization state due to the weaker magnetic field, while the reluctance torque still exists. The corresponding torque waveforms at the current angle of 0° and the current angle exhibiting the highest torque respectively are presented in Fig. 9. Furthermore, in the fully forward magnetization state, the average torque versus i_q is illustrated in Fig. 10, albeit with the average torque versus current amplitude under the current angle exhibiting the highest torque at each point. It can be seen that the ratio of the reluctance torque to the overall torque increases with the increasing of current amplitudes.

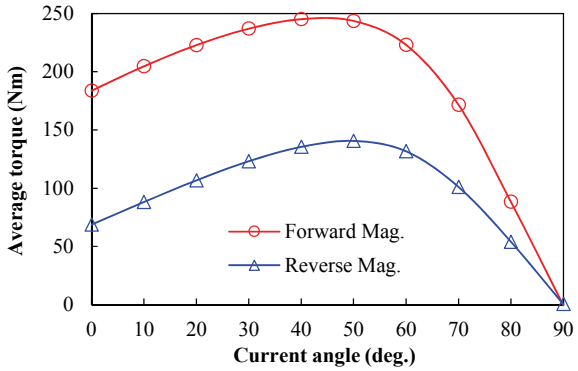

Fig. 8 Average torque versus current angle in fully forward and reverse magnetization states.

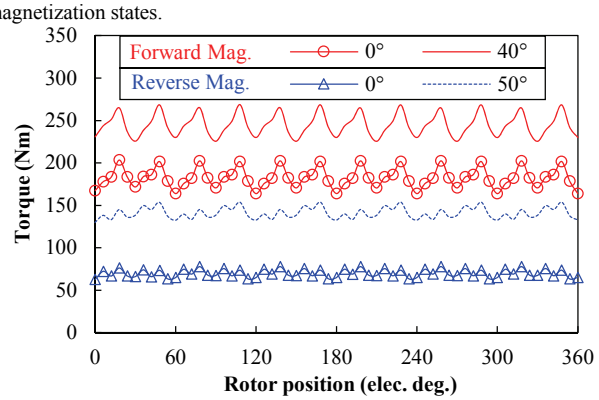

Fig. 9 Torque waveforms in fully forward and reverse magnetization states.

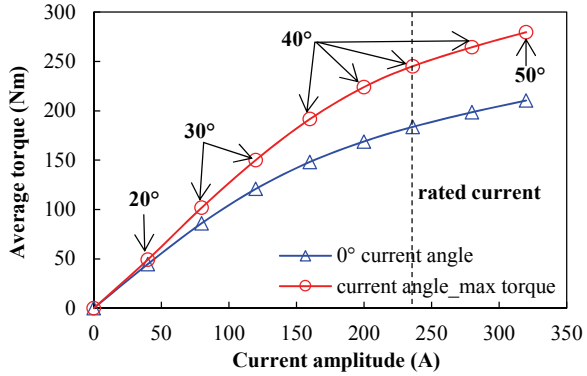

Fig. 10 Average torque versus current amplitude with different current angle in the fully forward magnetization states.

IV. Demagnetization and Magnetization

The demagnetization and magnetization of VPMs should be investigated, which are always challenging, especially for rotor-PM VFM machines without field windings [6], [9], [16], [18].

A. Unintentional demagentization with i_q

The VFM machines should withstand the unintentional demagnetization caused by i_q. Thanks to the assistance of CPMs, the proposed series hybrid PM VFM machine can keep the working point of VPM unaffected by i_q. Fig. 11

depicts the fundamental back-EMFs at 1500 r/min after different i_q excitations, based on the fully forward magnetization state. The back-EMFs only have a slight drop even when the current is very high.

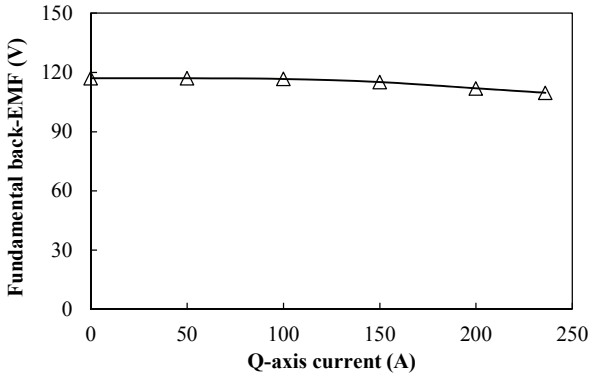

Fig. 11 Peak fundamental phase back-EMFs at 1500 r/min after different i_q excitations from fully forward magnetization state.

B. Demagentization and magnetization with i_d

The demagnetization from the fully forward magnetization and the re-magnetization from the fully reverse magnetization are illustrated in Fig. 12, where the fundamental back-EMFs after $-i_d$ (demagnetization) and $+i_d$ (re-magnetization) are presented. The VPMs can be entirely demagnetized to the opposite polarity based on the fully forward magnetization state, when an approximately 3 times rated current is applied. Afterwards, the full re-magnetization can be obtained if an around 6 times rated current is injected.

The magnetization characteristics of the VPM during demagnetization and magnetization are investigated and presented in Fig. 13, in which the working points of the VPM are specified. Initially, in the fully forward magnetization state, the open-circuit working point of the VPM locates at point M, which is among the stable region on the demagnetization curve. Then, the working point would move below the knee point with i_d=-150A, and the irreversible demagnetization happens. Moreover, the working points decline continuously along the demagnetization curve in Quadrants II and III with $-i_d$ increasing, and the VPM would be fully demagnetized if i_d=-2000A is applied. It should be noted that this current is much higher than the required current for fully demagnetization which is demonstrated previously, which will be explained as follows.

The VPM working point locates at point N in the fully reverse magnetization state. The VPM already has been partially re-magnetized by the CPM under the open-circuit conditions, since the magnetization polarities of VPM and CPM are inherently opposite when the VPM operates in the reverse magnetization state. With the increase of $+i_d$, the VPM working points ascend continuously. The full magnetization can be obtained with $+i_d$=1600A. Once the VPM has been fully re-magnetized, the working point would return to point M after the current is released. Hence, the VPM working point is flexibly adjusted by applying different i_d, with which the variation of PM flux is achieved.

The re-magnetization of the VPM is facilitated by the CPM in the proposed VFM machine, but it is still challenging since the magnetic saturation is severe during magnetization. On the other hand, with the aid of the CPM, the VPM is difficult to be demagnetized, even when $-i_d$ is applied for the intentional demagnetization. Nevertheless, it is actually not necessary to demagnetize the VPM to the lowest working point by i_d=-2000A, since it would automatically shift to point N due to the re-magnetization of CPM. Therefore, it is enough to demagnetize the VPM to the working point P, with which it would automatically move to point N along the recoil line PN after the current is released. As a result, the full demagnetization has been realized as well whilst the required current is remarkably reduced.

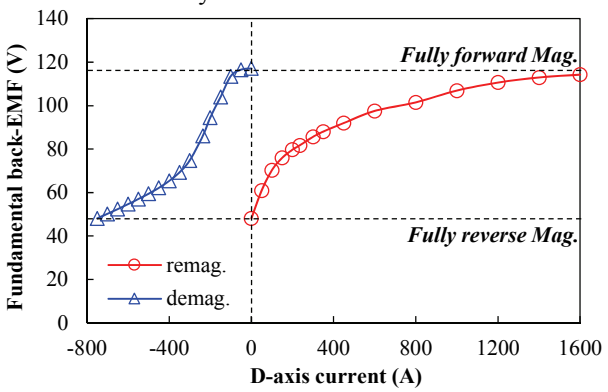

Fig. 12 Peak fundamental phase back-EMFs at 1500 r/min after different positive and negative i_d excitations.

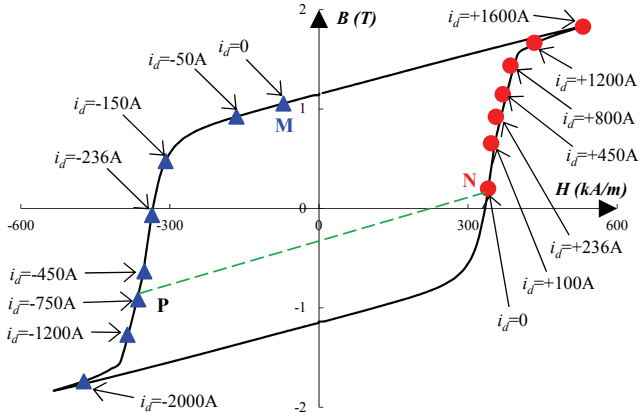

Fig. 13 Working points of the VPM during demagnetization and magnetization.

In order to further demonstrate the magnetic characteristics in the demagnetization and re-magnetization, a monitoring line AB inside the VPM is employed, as illustrated in Fig. 1. It should be noted that the two pieces of VPMs in one rotor pole are symmetrical when i_d is applied. The flux densities along the magnetization direction on the monitoring line AB after demagnetization and re-magnetization are shown in Figs. 14(a) and (b) respectively. i_d=-750A can approximately fully demagnetized the VPMs based on the fully forward state, and i_d=+1600A can make the VPMs back to the fully forward state again. However, it should be noted that the VPM portions close to d-axis position are easy to be demagnetized or re-magnetized by i_d while the portions close to q-axis position are difficult to be affected. As a result, the uneven field distributions inside the VPMs may occur if they are not fully demagnetized or fully re-magnetized, with which the spatial harmonics and local saturation could be increased, degrading the machine performance.

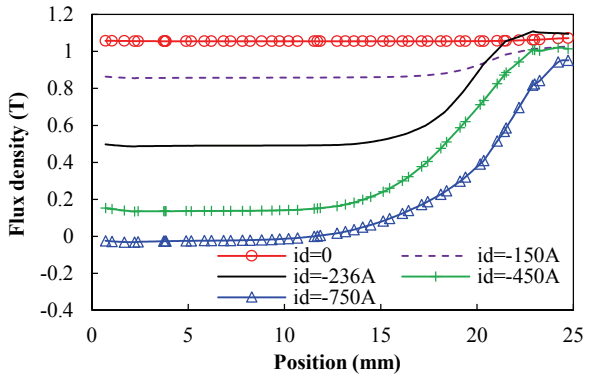

(a) Demagnetization from fully forward magnetization state

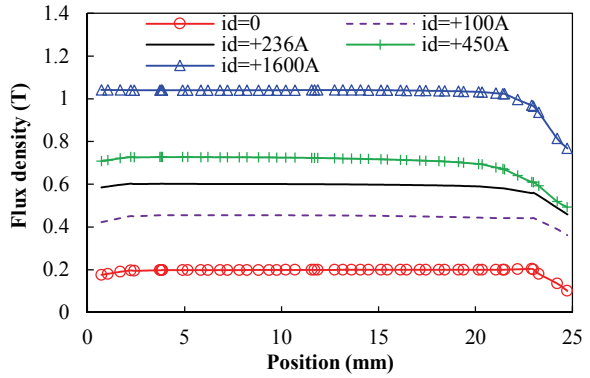

(b) Re-magnetization from fully reverse magnetization state

Fig. 14 Flux densities in the central line inside the VPM after demagnetization and re-magnetization.

In the previous analysis, it is revealed that the VPMs can be magnetized or demagnetized with the appropriate i_d, and the full magnetization and demagnetization states are obtained if i_d is high enough. The magnetic saturation has a significant influence on the required demagnetizing and magnetizing currents, since the severe saturation occurs with a high i_d applied. It should be mentioned that the full flux variation range is not always necessary, while a relatively narrower variation range may be employed and hence the required demagnetizing and magnetizing currents can be reduced. With the 450A current limit in the study system, the VPMs can be demagnetized to exhibit the fundamental back-EMF of around 63V, as shown in Fig. 12, which is 54% compared to the back-EMF in the full forward magnetization state (54% magnetization state).

V. Efficiency Improvement

A major benefit of VFM machines is the elimination of the continuous $-i_d$ during high speed operation, which leads to higher efficiency. Therefore, it is useful to investigate the efficiency performance of the proposed series hybrid PM VFM machine. With the bus voltage of 650V and current limit of 236A, the efficiency map of the proposed VFM machine is predicted. The iron losses and copper losses with different currents are swept based on FE method, and the optimum efficiency at each operation point is obtained [25].

Figs. 15(a) and (b) illustrate the efficiency maps in the fully forward and the 54% magnetization states respectively. It can be observed that the higher torque output is obtained in the fully forward magnetization state, and the efficiency is high in the low speed-high torque region. In contrast, although the torque output is sacrificed in the 54% magnetization state, the efficiency in the high speed-low torque region is significantly improved. Consequently, it is beneficial to flexibly switch the magnetization state at different operation regions, e.g. full magnetization during high torque region while partial magnetization during high speed region. As a result, a new efficiency map combining the advantages can be obtained, as shown in Fig. 15(c).

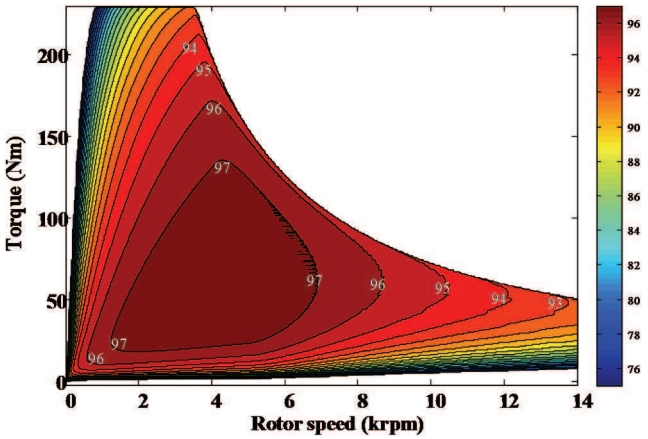

(a) In the fully forward magnetization state

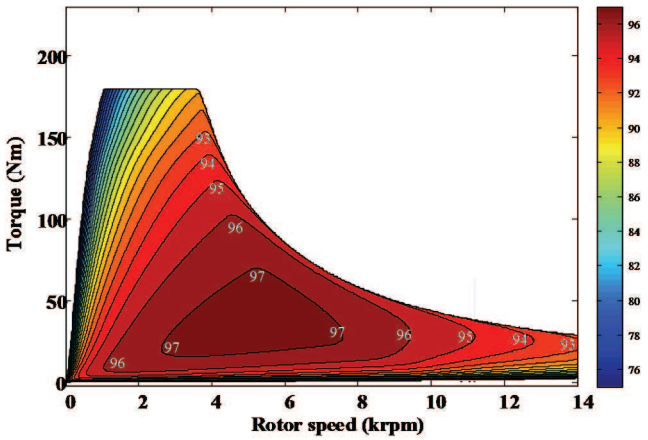

(b) In the 54% magnetization state

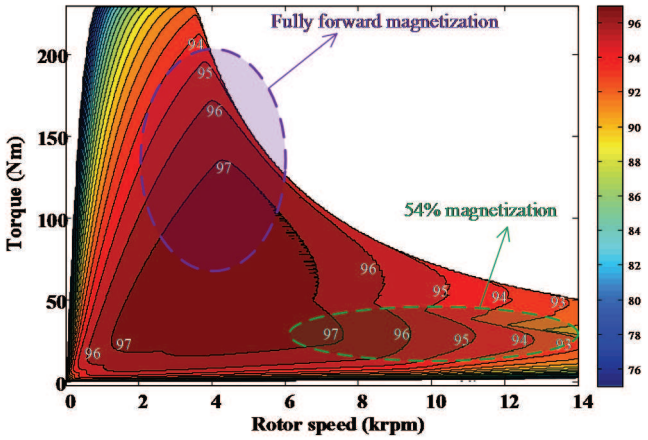

(c) Integration of the two magnetization states

Fig. 15 Efficiency maps in different magnetization states.

VI. Experimental Validation

In order to validate the previous analysis on the proposed VFM machine, a prototype machine is manufactured and tested. The key design parameters of the fabricated prototype machine are listed in Table I, and the essential components are presented in Fig. 16. The stator of the Prius2010 IPM machine has been directly employed, but the rotor is distinct. The NdFeB PMs have been fully magnetized before fitting into the rotor, while the non-magnetized SmCo PMs are

employed, which implies the post-assembly magnetization is required for SmCo PMs.

The test platform is shown in Fig. 17. The positive i_d =450A, which is the maximum available current of the inverter, is firstly applied to magnetize the VPMs. Then, the open-circuit back-EMF and torque output are measured. The 3-D FE simulations are employed to consider the end effect. Fig. 18 shows the FE-predicted and measured phase back-EMFs at 1500 r/min after i_d=450A magnetization (maximum available magnetization state), and a relatively good agreement can be observed between the measured and 3-D FE results. Furthermore, with i_d =0 control strategy, the average torques with different i_q are measured and compared to the FE predictions in Fig. 19. The measured results agree with the 3-D FE predictions. Moreover, it is important to verify the reluctance torque of the proposed machine, to which both i_d and i_q components should be applied. Fig. 20 shows the dynamic torque waveforms with both i_d and i_q components. With the almost constant i_q, the resultant torque remarkably increases when i_d is applied, which reveals that the reluctance torque makes a significant contribution to the torque output. In addition, the 2-D FE-predicted torques based on the corresponding currents are presented as well, in which the FE results agree well with the measured results.

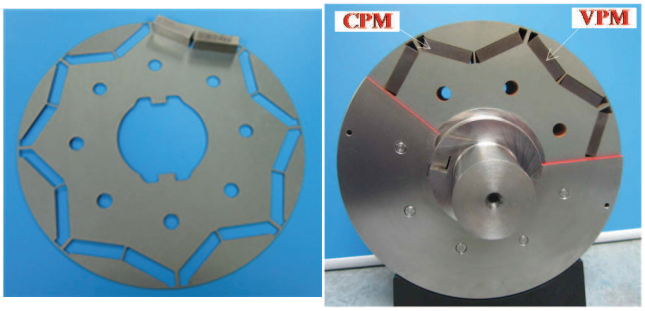

(a) Rotor lamination (b) Assembled rotor

(c) Stator (d) Rotor fitting in stator

Fig. 16 Prototype of the proposed series hybrid PM VFM machine.

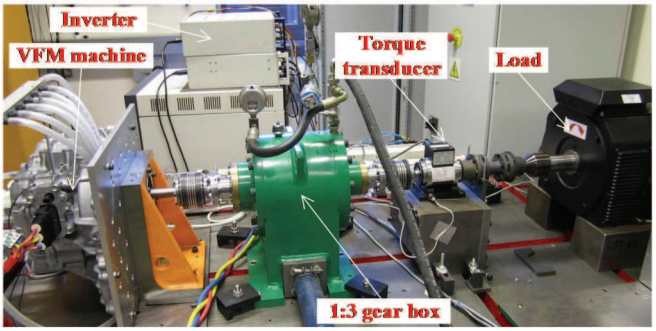

Fig. 17 Test platform for torque measurement.

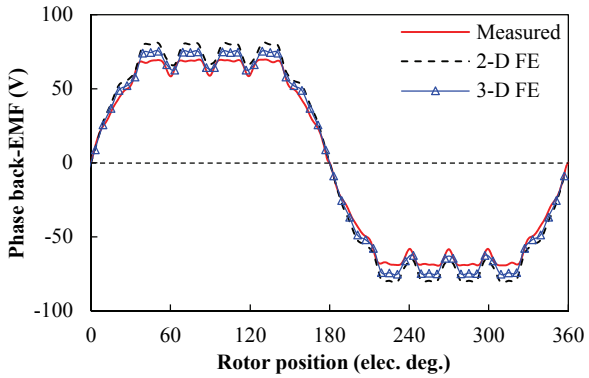

Fig. 18 Measured and 2-D, 3-D FE-predicted phase back-EMFs at 1500 r/min in the maximum available magnetization state.

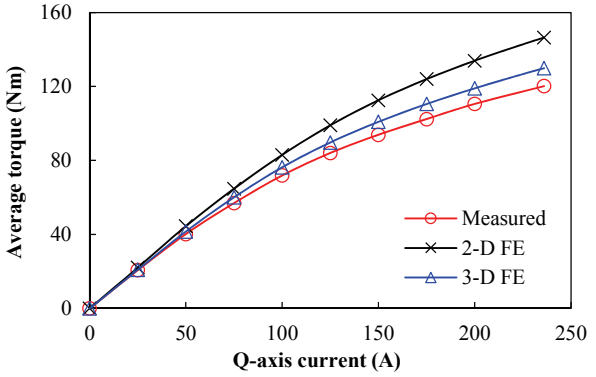

Fig. 19 Measured and 2-D, 3-D FE-predicted average torques versus i_q in the maximum available magnetization state.

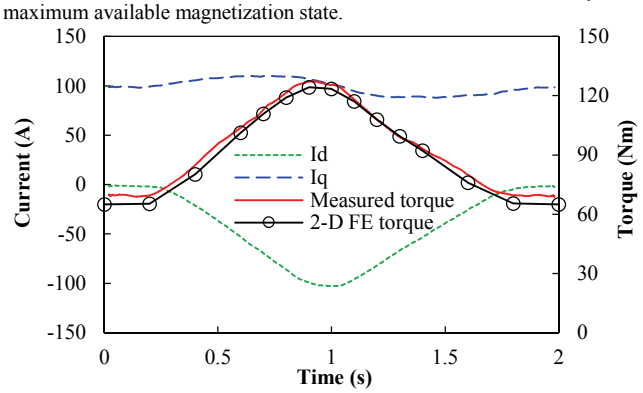

(a) With maximum i_q =100A, i_d = -100A

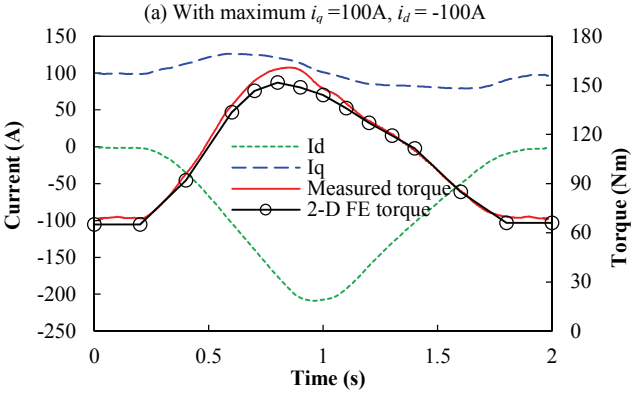

(a) With maximum i_q =100A, i_d = -100A

Fig. 20 Measured and 2-D FE-predicted dynamic torque waveforms with both i_q and i_d components.

VII. Conclusions

In this paper, a novel series hybrid PM VFM machine is introduced, which overcomes the drawback of sacrificed torque density in the conventional VFM machines. The VPMs and CPMs are alternatively placed on adjacent rotor poles, and thus two sets of PMs are magnetically connected in series. The working point of VPMs is stable even if $-i_d$ is

applied, as the CPM flux can assist the VPMs. Therefore, it is safe to employ a high current. Moreover, the reluctance torque is regained when the IPM rotor and full-pitched armature windings are employed. Thus, the torque density is remarkably improved (as high as 80kNm/m^3). Further, it has revealed that the machine efficiency can be increased by flexibly adjusting the PM magnetization state. However, it can be noted that the required demagnetizing and re-magnetizing currents are relatively high in the prototype machine, which exceed the current rating of the inverter and thus limit the performance. In the future work, a comprehensive design of the machine should be carried out to relieve the magnetic saturation and reduce the required currents. The directly inherited stator from the Prius2010 IPM machine should be modified, and more importantly, the PM dimensions should be optimized, together with the selection of the most appropriate VPM material.

REFERENCES

[1] Z.Q. Zhu and D. Howe, "Electrical machines and drives for electric, hybrid, and fuel cell vehicles," *Proc. IEEE*, vol. 95, no. 4, pp. 746-765, Apr. 2007.

[2] K.T. Chau, C.C. Chan, and C. Liu, "Overview of permanent-magnet brushless drives for electric and hybrid electric vehicles," *IEEE Trans. Ind. Electron.*, vol. 55, no. 6, pp. 2246-2257, Jun. 2008.

[3] T.M. Jahns, G. Kliman, and T. Neumann, "Interior Permanent-magnet synchronous motors for adjustable-speed drives," *IEEE Trans. Ind. Appl.*, vol. IA-22, no. 4, pp. 738-747, Jul./Aug. 1986.

[4] W.L. Song and T.J. Miller, "Field-weakening performance of brushless synchronous AC motor drives," *IEE Proc. Electr. Power Appl.*, vol. 141, no. 6, pp. 331-340, Nov. 1994.

[5] B. Chalmers, L. Musaba, and D. Gosden, "Variable-frequency synchronous motor drives for elelctric vehicles," *IEEE Trans. Ind. Appl.*, vol. 32, no. 4, pp. 896-903, Jul./Aug. 1996.

[6] N. Bianchi, S. Bolognani, and B. Chalmers, "Salient-rotor PM synchronous motors for an extended flux-weakening operation range," *IEEE Trans. Ind. Appl.*, vol. 36, no. 4, pp. 1118-1125, Jul./Aug. 2000.

[7] V. Ostovic, "Memory motors – a new class of controllable flux PM machines for a true wide speed operation," in *Proc. Ind. Appl. Conf. (IAS) Ann. Meeting*, Sep. 30- Oct. 04, 2001, vol. 4, pp. 2577-2584.

[8] V. Ostovic, "Memory motors," *IEEE Magn. Ind. Appl.*, vol. 9, no. 1, pp. 52-61, Jan./Feb. 2003.

[9] N. Limsuwan, T. Kato, K. Akatsu, and R.D. Lorenz, "Design and evaluation of a variable-flux flux-intensifying interior permanent magnet machine," in *Proc. Energy Convers. Cong. Expo. (ECCE)*, Sep. 2012, pp. 3670-3677.

[10] T. Kato, N. Limsuwan, C. Yu, K. Akatsu, and R.D. Lorenz, "Rare earth reduction using a novel variable magnetomotive force flux-intensified IPM machine," *IEEE Trans. Ind. Appl.*, vol. 50, no. 3, pp. 1748-1756, May/Jun. 2014.

[11] T. Fukushige, N. Limsuwan, T. Kato, K. Akatsu, and R.D. Lorenz, "Efficiency contours and loss minimization over a driving cycle of a variable-flux flux-intensifying interior machine," *IEEE Trans. Ind. Appl.*, vol. 51, no. 4, pp. 2984-2989, Jul./Aug. 2015.

[12] M. Ibrahim, L. Masisi, and P. Pillay, "Design of variable-flux permanent-magnet machines using Alnico magnets," *IEEE Trans. Ind Appl.*, vol. 51, no. 6, pp. 4482-4491, Nov./Dec. 2015.

[13] M. Ibrahim, L. Masisi, and P. Pillay, "Design of variable flux permanent-magnet machine for reduced inverter rating," *IEEE Trans. Ind. Appl.*, vol. 51, no. 5, pp. 3666-3674, Sep./Oct. 2015.

[14] Y. Gong, K. T. Chau, J. Z. Jiang, C. Yu, and W. Li, "Analysis of doubly salient memory motors using preisach theory," *IEEE Trans. Magn.*, vol. 45, no. 10, pp. 4676-4679, Oct. 2009.

[15] X. Zhu, L. Quan, D. Chen, M. Cheng, Z. Wang, and W. Li, "Design and analysis of a new flux memory doubly salient motor capable of online flux control," *IEEE Trans. Magn.*, vol. 47, no. 10, pp. 3220-3223, Oct. 2011.

[16] H. Yang, H. Lin, J. Dong, J. Yan, Y. Huang, S. Fang, "Analysis of a novel switched-flux memory motor employing time-divisional magnetization strategy," *IEEE Trans. Magn*, vol. 50, no. 2, pp. 7021004, Feb. 2014.

[17] D. Wu, X. Liu, Z.Q. Zhu, A. Pride, R. Deodhar, and T. Sasaki, "Switched flux hybrid magnet memory motor,". *IET Proc Elec. Power Appl*., vol. 9, no. 2, pp.160-170, Feb. 2015.

[18] Y. Chen, W. Pan, Y. Wang, R. Tang, and J. Wang, "Interior composite-rotor controllable-flux PMSM-memory motor," in *Proc. Inter. Conf. Elec. Mach. System. (ICEMS)*, Sep. 2005, vol. 1, pp. 446-449.

[19] K. Sakai, K. Yuki, Y. Hashiba, N. Takahashi, and K. Yasui, "Principle of the variable-magnetic-force memory motor," in *Proc. Inter. Conf. Elec. Mach. System. (ICEMS)*, Nov. 2009, pp. 1-6.

[20] Y. Zhou, Y. Chen, and J. X. Shen, "Analysis and improvement of a hybrid permanent magnet memory motor," *IEEE Trans. Energy Convers.*, vol. 31, no. 3, pp. 915-923, Sep. 2016.

[21] D. Wu, Z.Q. Zhu, X. Liu, A. Pride, R. Deodhar, and T. Sasaki, "Cross coupling effect in hybrid magnet memory motor," in *Proc. Inter. Conf. Power Elec. Mach. and Drives (PEMD)*, Apr. 2014, pp. 1-6.

[22] S. Maekawa, K. Yuki, M. Matsushita, I. Nitta, Y. Hasegawa, and T. Shiga, "Study of the magnetization method suitable for fractional-slot concentrated-winding variable magnetomotive-force memory motor," *IEEE Trans. Power Electron.*, vol. 29, no. 9, pp. 4877-4887, Sep. 2014.

[23] J. Kim, J. Choi, K. Lee, and S. Lee, "Design and analysis of surface-mounted-type variable flux permanent magnet motor for wide-speed range applications," *IEEE Trans. Magn.*, vol. 51, no. 11, pp. 8111004, Nov. 2015.

[24] H. Hua, Z.Q. Zhu, A. Pride, R. Deodhar, and T. Sasaki, "A novel variable flux memory machine with series hybrid magnets," in Proc. *Energy Convers. Cong. Expo. (ECCE)*, Sep. 18-22, 2016, pp. 1-8.

[25] W. Chu, Z.Q. Zhu, J. Zhang, X. Liu, D. Stone, and M. Foster, "Investigation on operational envelops and efficiency maps of electrically excited machines for electrical vehicle applications," *IEEE Trans. Magn.*, vol. 51, no. 4, pp. 8103510, Apr. 2015.

Hao Hua (S'15) was born in Hefei, China, in 1990. He received the M.Sc. degree in electrical engineering from Southeast University, Nanjing, China, in 2014. He is currently working toward the Ph.D. degree at The University of Sheffield, Sheffield, U.K.

His major research interests include the design and analysis of permanent-magnet and hybrid-excited machines for applications in automotive and renewable energy.

Z.Q. Zhu (M'90–SM'00–F'09) received the B.Eng. and M.Sc. degrees in electrical and electronic engineering from Zhejiang University, Hangzhou, China, in 1982 and 1984, respectively, and the Ph.D. degree in electrical and electronic engineering from The University of Sheffield, Sheffield, U.K., in 1991.

Since 1988, he has been with the University of Sheffield, where he is currently a Professor with the Department of Electronic and Electrical Engineering and the Head of the Electrical Machines and Drives Research Group. He is a Fellow of Royal Academy of Engineering, U.K. His current major research interests include the design and control of permanent-magnet brushless machines and drives for applications ranging from automotive to renewable energy.

Adam Pride (M'97) received the B.Sc. and M.Sc. degrees in electrical engineering from the University of Manchester Institute of Science and Technology (now the University of Manchester), Manchester, U.K., in 1977 and 1979, respectively.

He was with Froude Consine Ltd., Worcester, U.K., where he worked on research and development of eddy-current dynamometers for automotive engine testing. In 1989, he took part in a four-year around-the-world sailing trip via the Atlantic and Pacific oceans on a 50-foot schooner. Since 1995, he has been with the U.K. Research Centre, IMRA Europe SAS, Brighton, U.K., where he has worked on a wide range of motors and actuators for automotive applications. He has co-authored 28 academic papers and has 19 patents. His particular interests include Halbach

magnetized permanent-magnet (PM) machines and analysis of optimum slot/pole combinations for concentrated winding PM machines.

Mr. Pride was awarded with a Silver Medal in the Worshipful Company of Turners/IMechE 1988 Engineering Design Competition for a fast-response motoring/absorbing dynamometer.

Rajesh P. Deodhar (M'89–S'94–SM'01) received the B.Eng. degree from University of Mumbai, India, in 1989, the M.Tech. degree from Centre for Electronics Design and Technology, Indian Institute of Science, Bangalore, India, in 1991, both in electronics engineering, and the Ph.D. degree from University of Glasgow, Scotland, U.K., in 1996.

Being a co-author for over one hundred publications at international conferences and peer-reviewed journals, and being a named inventor or co-inventor for over 40 international patent (applied or granted) documents, and with research assignments at Crompton Greaves Ltd. in India, Hitachi Ltd. in Japan, and the Scottish Power Electronics and Electric Drives Laboratory at University of Glasgow in the U.K., Dr. Deodhar has a substantial and a global research profile in the field of electric machines and drives. In 1998, he joined IMRA Europe SAS U.K. Research Centre, Brighton, U.K., where he currently serves as Project Manager working on the design and analysis of a wide range of motors and actuators used in automotive components and systems.

Dr. Deodhar has received numerous awards, including the Indian Institute of Science Gold Medal in 1991, the IEEE Industry Applications Society Electric Machines Committee first prize paper Award in 1996, the IEEE Transactions on Industry Applications second prize paper Award in 1998. More recently, he has been a prize paper award recipient at the IEEE international conferences in 2010, 2012 and 2014. He serves as a reviewer for a number of IEEE journals and as a Technical Planning Committee member for a number of international conferences, and, is a past Associate Editor for the IEEE Transactions on Industry Applications. He is a Chartered Engineer and a Fellow of the Institution of Engineering and Technology in the U.K.

Toshinori Sasaki received the B.Sc. degree in mechanical from the University of Okayama, Japan, in 1985. After graduation, he joined Aisin Seiki Co. in Japan, where he has worked in various technical and management roles over past 30 years.

Mr. Sasaki gained additional overseas experience by working at the Aisin Technical Centre of America (ATCA). Since 2014, he has served as the General Manager of IMRA Europe SAS UK Research Centre at Brighton UK, where he oversees the development of advanced far-future automotive technologies.